

# Interpreting cancer genomes using systematic host network perturbations by tumour virus proteins

Orit Rozenblatt-Rosen<sup>1,2,3\*</sup>, Rahul C. Deo<sup>1,4,5\*</sup>, Megha Padil<sup>1,6,7\*</sup>, Guillaume Adelmant<sup>1,4,8\*</sup>, Michael A. Calderwood<sup>1,9,10,11</sup>, Thomas Rolland<sup>1,9,10</sup>, Miranda Grace<sup>1,12</sup>, Amélie Dricot<sup>1,9,10</sup>, Manor Askenazi<sup>1,4,8</sup>, Maria Tavares<sup>1,2,3,8</sup>, Samuel J. Pevzner<sup>9,10,13</sup>, Fieda Abderazzaq<sup>1,6</sup>, Danielle Byrdsong<sup>1,9,10</sup>, Anne-Ruxandra Carvunis<sup>9,10</sup>, Alyce A. Chen<sup>1,12</sup>, Jingwei Cheng<sup>2,3</sup>, Mick Correll<sup>6</sup>, Melissa Duarte<sup>1,9,11</sup>, Changyu Fan<sup>1,9,10</sup>, Mariet C. Feltkamp<sup>14</sup>, Scott B. Ficarro<sup>1,4,8</sup>, Rachel Franchi<sup>1,9,15</sup>, Brijesh K. Garg<sup>1,4,8</sup>, Natali Gulbahce<sup>1,9,16,17</sup>, Tong Hao<sup>1,9,10</sup>, Amy M. Holthaus<sup>1,11</sup>, Robert James<sup>1,9,10</sup>, Anna Korkhin<sup>1,2,3</sup>, Larisa Litovchick<sup>1,2,3</sup>, Jessica C. Mar<sup>1,6,7</sup>, Theodore R. Pak<sup>18</sup>, Sabrina Rabello<sup>1,3,9,16</sup>, Renee Rubio<sup>1,6</sup>, Yun Shen<sup>1,9,10</sup>, Saurav Singh<sup>4,8</sup>, Jennifer M. Spangle<sup>1,12</sup>, Murat Tasan<sup>1,4,18</sup>, Shelly Wanamaker<sup>9,10,15</sup>, James T. Webber<sup>4,8</sup>, Jennifer Roecklein-Canfield<sup>9,15</sup>, Eric Johannsen<sup>1,11</sup>, Albert-László Barabási<sup>1,3,9,16</sup>, Rameen Beroukhi<sup>3,19,20</sup>, Elliott Kieff<sup>1,11</sup>, Michael E. Cusick<sup>1,9,10</sup>, David E. Hill<sup>1,9,10</sup>, Karl Münger<sup>1,12</sup>, Jarrod A. Marto<sup>1,4,8</sup>, John Quackenbush<sup>1,6,7</sup>, Frederick P. Roth<sup>1,4,9,18</sup>, James A. DeCaprio<sup>1,2,3</sup> & Marc Vidal<sup>1,9,10</sup>

**Genotypic differences greatly influence susceptibility and resistance to disease. Understanding genotype–phenotype relationships requires that phenotypes be viewed as manifestations of network properties, rather than simply as the result of individual genomic variations<sup>1</sup>. Genome sequencing efforts have identified numerous germline mutations, and large numbers of somatic genomic alterations, associated with a predisposition to cancer<sup>2</sup>. However, it remains difficult to distinguish background, or ‘passenger’, cancer mutations from causal, or ‘driver’, mutations in these data sets. Human viruses intrinsically depend on their host cell during the course of infection and can elicit pathological phenotypes similar to those arising from mutations<sup>3</sup>. Here we test the hypothesis that genomic variations and tumour viruses may cause cancer through related mechanisms, by systematically examining host interactome and transcriptome network perturbations caused by DNA tumour virus proteins. The resulting integrated viral perturbation data reflects rewiring of the host cell networks, and highlights pathways, such as Notch signalling and apoptosis, that go awry in cancer. We show that systematic analyses of host targets of viral proteins can identify cancer genes with a success rate on a par with their identification through functional genomics and large-scale cataloguing of tumour mutations. Together, these complementary approaches increase the specificity of cancer gene identification. Combining systems-level studies of pathogen-encoded gene products with genomic approaches will facilitate the prioritization of cancer-causing driver genes to advance the understanding of the genetic basis of human cancer.**

Integrative studies of viral proteins have identified host perturbations relevant to the aetiology of viral disease<sup>4,5</sup>. We examined whether such a strategy, extended systematically across a range of tumour viruses, could shed light on cancers even beyond those directly caused by these pathogens. Our hypothesis is inspired by classical examples in

which DNA tumour virus proteins physically target the products of *RBI* or *TP53*, two well-established germline-inherited and somatically inactivated tumour-suppressor genes<sup>6</sup>. We propose that viruses and genomic variations alter local and global properties of cellular networks in similar ways to cause pathological states. Models derived from host perturbations mediated by viral proteins representing the virome<sup>7</sup> should serve as surrogates for network perturbations that result from large numbers of genomic variations, or the variome<sup>8</sup> (Fig. 1a).

We developed an integrated pipeline to systematically investigate perturbations of host interactome and transcriptome networks induced by gene products of four functionally related, yet biologically distinct, families of DNA tumour viruses: human papillomavirus (HPV), Epstein–Barr virus (EBV), adenovirus (Ad5) and polyomavirus (PyV) (Fig. 1b, Supplementary Table 1 and Supplementary Fig. 1).

Applying a stringent implementation of the yeast two-hybrid (Y2H) system<sup>9</sup>, 123 viral open reading frames (viral ORFs) were screened against a collection of about 13,000 human ORFs<sup>10</sup>, resulting in a validated virus–host interaction network of 454 binary interactions involving 53 viral proteins and 307 human proteins (Fig. 1c and Supplementary Table 2). Analysis of our binary interaction map identified 31 host target proteins that showed more binary interactions with viral proteins than would be expected given their ‘degree’ (number of interactors) in our current binary map of the human interactome network (HI-2)<sup>11</sup> (Fig. 1c, Supplementary Table 3 and Supplementary Notes), suggesting a set of common mechanisms by which different viral proteins rewire the host interactome network.

To examine perturbations in both the interactome and transcriptome networks directly in human cells, we generated expression constructs fusing each viral ORF to a tandem epitope tag and introduced each construct into IMR-90 normal human diploid fibroblasts. Interactions between viral proteins and the host proteome were identified by tandem affinity purification followed by mass spectrometry (TAP–MS)<sup>12</sup>. The

<sup>1</sup>Genomic Analysis of Network Perturbations Center of Excellence in Genomic Science, Center for Cancer Systems Biology (CCSB), Dana-Farber Cancer Institute, Boston, Massachusetts 02215, USA.

<sup>2</sup>Department of Medical Oncology, Dana-Farber Cancer Institute, Boston, Massachusetts 02215, USA. <sup>3</sup>Department of Medicine, Brigham and Women’s Hospital, Harvard Medical School, Boston, Massachusetts 02115, USA. <sup>4</sup>Department of Biological Chemistry and Molecular Pharmacology, Harvard Medical School, Boston, Massachusetts 02115, USA. <sup>5</sup>Cardiovascular Research Institute, Department of Medicine and Institute for Human Genetics, University of California, San Francisco, California 94143, USA. <sup>6</sup>Center for Cancer Computational Biology (CCCB), Department of Biostatistics and Computational Biology and Department of Cancer Biology, Dana-Farber Cancer Institute, Boston, Massachusetts 02215, USA. <sup>7</sup>Department of Biostatistics, Harvard School of Public Health, Boston, Massachusetts 02115, USA. <sup>8</sup>Blais Proteomics Center and Department of Cancer Biology, Dana-Farber Cancer Institute, Boston, Massachusetts 02215, USA. <sup>9</sup>Center for Cancer Systems Biology (CCSB) and Department of Cancer Biology, Dana-Farber Cancer Institute, Boston, Massachusetts 02215, USA. <sup>10</sup>Department of Genetics, Harvard Medical School, Boston, Massachusetts 02115, USA. <sup>11</sup>Infectious Diseases Division, The Channing Laboratory, Brigham and Women’s Hospital and Departments of Medicine and of Microbiology and Immunobiology, Harvard Medical School, Boston, Massachusetts 02115, USA. <sup>12</sup>Division of Infectious Diseases, Brigham and Women’s Hospital and Department of Medicine, Harvard Medical School, Boston, Massachusetts 02115, USA. <sup>13</sup>Biomedical Engineering Department, Boston University and Boston University School of Medicine, Boston, Massachusetts 02118, USA. <sup>14</sup>Department of Medical Microbiology, Leiden University Medical Center, 2300 RC Leiden, The Netherlands. <sup>15</sup>Department of Chemistry, Simmons College, Boston, Massachusetts 02115, USA. <sup>16</sup>Center for Complex Networks Research (CCNR) and Department of Physics, Northeastern University, Boston, Massachusetts 02115, USA. <sup>17</sup>Department of Cellular and Molecular Pharmacology, University of California, San Francisco, California 94158, USA. <sup>18</sup>Donnelly Centre and Departments of Molecular Genetics and Computer Science, University of Toronto and Lunenfeld Research Institute, Mt Sinai Hospital, Toronto, Ontario M5G 1X5, Canada. <sup>19</sup>Department of Medical Oncology and Department of Cancer Biology, Dana-Farber Cancer Institute, Boston, Massachusetts 02215, USA. <sup>20</sup>The Broad Institute, Cambridge, Massachusetts 02142, USA.

\*These authors contributed equally to this work.

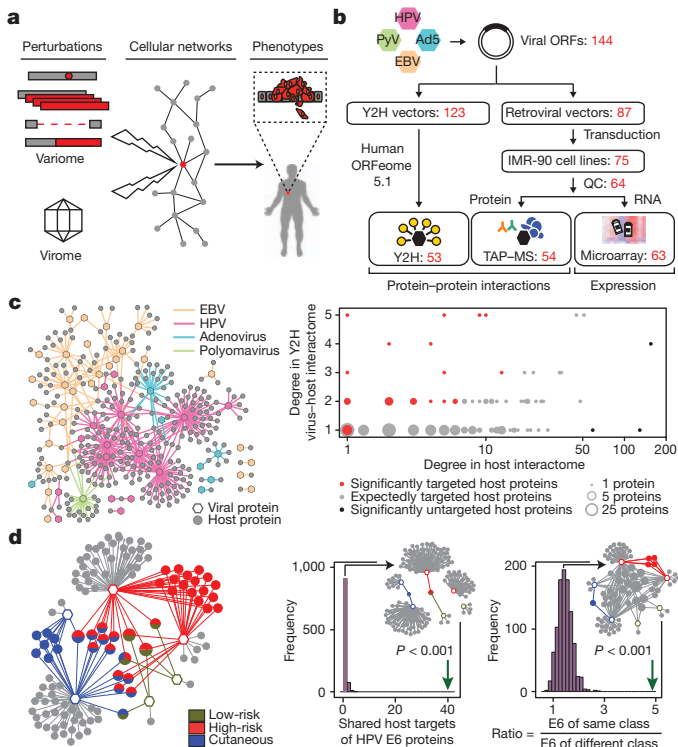


**Figure 1 | Systematic mapping of binary interactions and protein complex associations between viral and host proteins.** **a**, The virome-to-variome network model proposes that genomic variations (point mutations, amplifications, deletions or translocations) and expression of tumour virus proteins induce related disease states by similarly influencing properties of cellular networks. **b**, Experimental pipeline for identifying virus–host interactions. Selected cloned viral ORFs were subjected to Y2H screens and introduced into cell lines for both TAP–MS and microarray analyses. Numbers of viral ORFs that were successfully processed at each step are indicated in red. **c**, Left: network of binary virus–host interactions identified by Y2H. Right: subsets of human target proteins that have significantly more (red dots) or fewer (black dots) viral interactors than expected on the basis of their degree in HI-2. **d**, Network of protein complex associations of E6 viral proteins from six HPV types (hexagons, coloured according to disease class) with host proteins (grey circles). Host proteins that associate with two or more E6 proteins are coloured according to the disease class(es) of the corresponding HPV types. Circle size is proportional to the number of associations between host and viral proteins in the E6 networks. Distribution plots of 1,000 randomized networks and experimentally observed data (green arrows) for the number of host proteins targeted by two or more viral proteins in the corresponding sub-networks (left histogram), or the ratio of the probability that a host protein is targeted by viral proteins from the same class to the probability that it is targeted by viral proteins from different classes (right histogram). Insets: representative random networks from these distributions.

intersection of two independent TAP–MS experiments yielded 3,787 reproducibly mapped virus–host protein complex associations involving 54 viral proteins and the products of 1,079 host genes (Supplementary Table 4). Statistically significant overlaps between the Y2H and the TAP–MS data sets with a positive reference set of curated virus–host interactions were observed, supporting the quality of the interactome data sets (Supplementary Notes). Host proteins identified as binary interactors or as members of protein complexes showed a statistically significant overlap ( $P < 0.001$ ) and a statistically significant tendency to interact with each other in HI-2 ( $P < 0.001$ ), implying that host targets in the virus–host interactome maps tend to fall in the same ‘neighbourhood’ of the host network<sup>1</sup> (Supplementary Fig. 2). Our two complementary interactome data sets highlight specific host biological processes targeted by viral proteins (Supplementary Fig. 3).

To explore the specificity of virus–host relationships, we examined protein complex associations mediated by E6 proteins from six distinct

HPV types representing three different disease classes: high-risk mucosal, low-risk mucosal and cutaneous. E6 and E7 proteins encoded by high-risk mucosal HPVs are strongly oncogenic<sup>6</sup>. Multiple host proteins were found to associate with E6 proteins encoded by two or more different HPV types ( $P < 0.001$ ; Fig. 1d), including the known E6 target UBE3A (E6AP)<sup>13</sup>. Among these we observed a statistically significant subgroup of host proteins targeted only by E6 proteins from the same disease class ( $P < 0.001$ ). The transcriptional regulators CREB-binding protein (CREBBP) and EP300 were found to associate with E6 proteins from both cutaneous HPV types, but not with those from the mucosal classes. In contrast with E6 proteins, no group of host proteins showed class-specific targeting by HPV E7 proteins (Supplementary Fig. 4). These differential associations reflect how rewiring of virus–host interactome networks may relate to the aetiology of viral disease.

In addition to targeting protein–protein interactions, viral proteins also functionally perturb their hosts through downstream effects on gene expression. We profiled the transcriptome of the viral ORF-transduced cell lines to trace pathways through which viral proteins could alter cellular states. Model-based clustering of the 2,944 most frequently perturbed host genes identified 31 clusters, many of which were enriched ( $P < 0.01$ ) for specific Gene Ontology (GO) terms and Kyoto Encyclopedia of Genes and Genomes (KEGG) pathways (Fig. 2a and Supplementary Tables 5 and 6). To uncover transcription factor (TF) binding motifs enriched within the promoters or enhancers of the corresponding genes, a high-confidence map of predicted TF binding sites was generated by using information on cell-specific chromatin accessibility and consensus TF-binding motifs (Supplementary Fig. 5). We found a densely interconnected set of 92 TFs (Supplementary Fig. 6 and Supplementary Notes) that either associated with or were differentially expressed in response to viral proteins, and for which target genes were enriched in at least one cluster (Supplementary Fig. 7 and Supplementary Table 7).

The mean expression change of each cluster revealed three distinct groups of viral proteins (Fig. 2a): group I included low-risk and cutaneous HPV E6 proteins, group II contained most of the EBV proteins, and group III included high-risk HPV E6 and E7 proteins and polyomavirus proteins. Consistent with their ability to associate with RB1, group III viral proteins increased the expression of genes that are involved in cell proliferation and whose promoters are enriched in E2F binding sites (clusters C26 and C31). Steady-state levels of these genes are correlated with cellular growth phenotypes (Supplementary Fig. 8 and Supplementary Notes). Similarly, the decreased expression of the p53 signalling pathway probably reflects the ability of group III proteins to bind to and inactivate p53 (cluster C12).

To investigate additional pathways through which viral proteins perturb TFs to reprogram cellular states, we derived a detailed network model containing 58 viral proteins that perturb the activity of 86 TFs, which in turn potentially regulate 30 clusters (Supplementary Fig. 9). This model was predictive of downstream patterns of differential expression ( $P = 0.003$ ; Fig. 2b) and suggested ways in which viral proteins could regulate many of the biological hallmarks of cancer<sup>14</sup> (Supplementary Notes). For example, we found the regulation of several pathways involved in the response to DNA damage (Fig. 2b), including autophagy potentially through NFE2L2 (cluster C3)<sup>15</sup>, the NF- $\kappa$ B-mediated inflammatory response (cluster C23)<sup>16</sup>, and the type I interferon response through IRF-1 (cluster C24; Supplementary Fig. 5)<sup>17</sup>.

Specific disease outcomes of the three disease classes of HPV might reflect how their respective proteins perturb distinct functional groups of host proteins. Our protein complex interaction map revealed associations between E6 from cutaneous HPVs and Mastermind-like protein 1 (MAML1), EP300 and CREBBP. MAML1 forms a transcriptional activation complex that modulates the expression of Notch target genes in conjunction with the EP300 and CREBBP histone acetyltransferases, the RBPJ transcription factor and the intracellular domain (ICD) of the Notch receptor<sup>18</sup>. Our transcriptome profiling placed the cutaneous

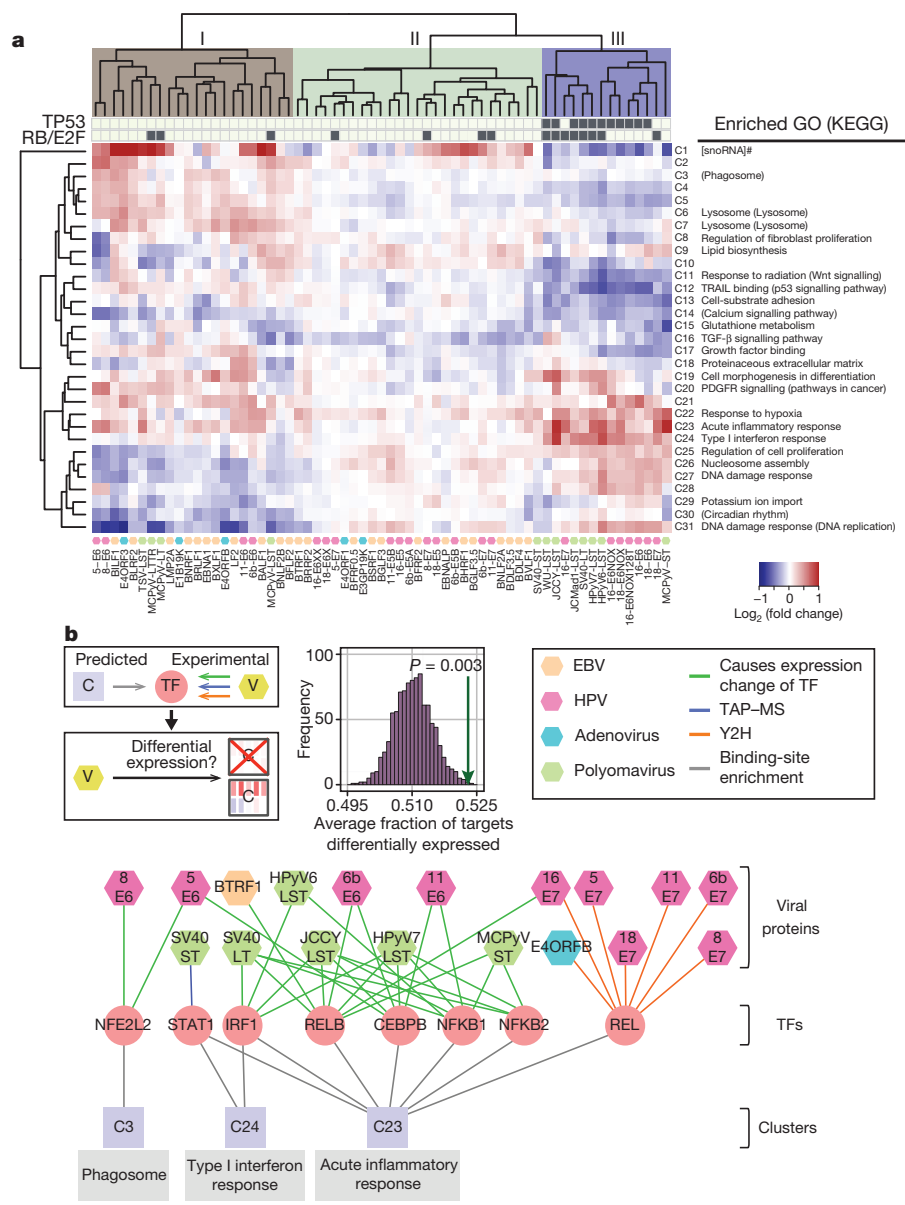


**Figure 2 | Transcriptome perturbations induced by viral protein expression.** **a**, Heat map of average cluster expression relative to control. Enriched GO terms and KEGG pathways are listed adjacent to the numbered expression clusters. In cluster C1, eight of the nine transcripts are the small nucleolar RNAs (denoted by hash mark). The upper dendrogram is shaded by viral ORF grouping. Grey blocks show which viral proteins associate with the

indicated host proteins. **b**, Diagram showing how the viral protein-TF-target gene network was constructed, with paths to three clusters shown. C, cluster; V, viral protein. Null distribution of average fraction of TF target genes differentially expressed in the corresponding cell lines (histogram), along with the observed value (green arrow).

and low-risk HPV E6 proteins in group I apart from the high-risk HPV E6 proteins in group III (Fig. 2a), so we investigated these differential perturbations. Both cutaneous HPV5 and HPV8 E6 proteins coprecipitated MAML1 and EP300, whereas the mucosal HPV E6 proteins did not (Fig. 3a and Supplementary Fig. 10); conversely, HPV6b, HPV11, HPV16 and HPV18 E6 proteins associated with UBE3A<sup>13</sup>, whereas cutaneous HPV E6 proteins did not.

Perturbations in Notch signalling can confer either oncogenic or tumour-suppressive effects<sup>18</sup>. Because both inhibition of the Notch pathway and the expression of HPV8 E6 promote squamous cell carcinoma<sup>19,20</sup>, we reasoned that binding of HPV5 and HPV8 E6 to MAML1 might inhibit Notch signalling. To test this, we examined transcript levels of Notch pathway genes and potential Notch target genes with a predicted RBPJ binding site in their promoter across all HPV E6 cell lines as well as in cells depleted for MAML1. Transcript levels of several Notch targets were significantly decreased in IMR-90

cells that were either depleted for MAML1 or expressing either HPV5 or HPV8 E6 (Fig. 3b and Supplementary Fig. 11). These and other results<sup>21</sup> indicate that the association of HPV5 and HPV8 E6 proteins with MAML1 inhibits Notch signalling. Building on these observations and on the established associations between EBV EBNA proteins and RBPJ<sup>22</sup>, we observed that viral proteins from all four DNA tumour viruses target proteins of the Notch pathway ( $P < 0.002$ ; Fig. 3c). Our data highlight the central role of Notch signalling in both virus-host perturbations and tumorigenesis, and support observations that implicate MAML1 in cancer pathogenesis<sup>23</sup>.

We next investigated the extent to which viral proteins globally target host proteins causally implicated in cancer. First we compared our viral targets, identified through binary interaction, protein complex associations and TF-binding-site analyses, against a gold standard set of 107 high-confidence causal human cancer genes in the COSMIC Classic (CC) gene set<sup>24</sup> (Supplementary Table 8). Viral targets were

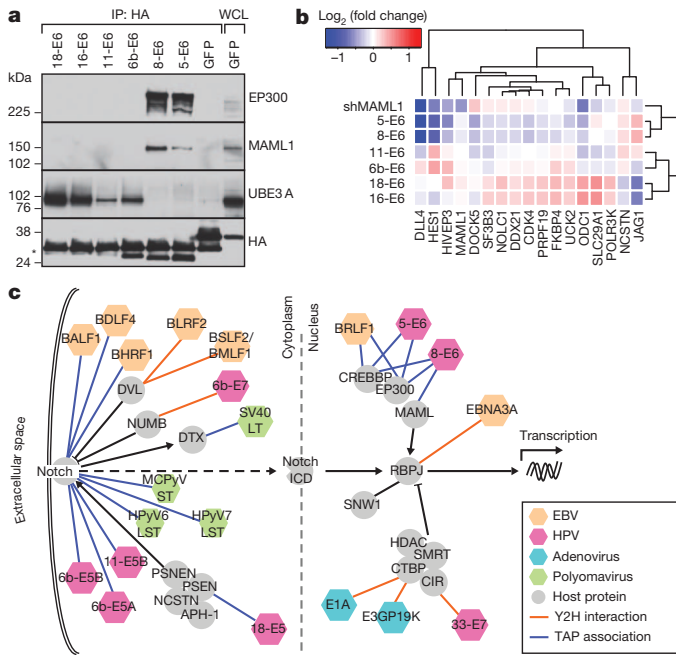


**Figure 3 | The Notch pathway is targeted by multiple DNA tumour virus proteins.** **a**, Western blots of co-immunoprecipitations of HPV E6 proteins in IMR-90 cells. **b**, Heat map of expression of Notch-pathway-responsive genes in IMR-90 cells on expression of E6 proteins from different HPV types or on knockdown of *MAML1*, relative to control cells. **c**, Representation of viral protein interactions with components of the Notch signalling pathway (as defined in KEGG). Notch ICD, Notch intracellular domain.

significantly enriched among CC genes (Supplementary Fig. 12; adjusted  $P$  for multiple hypothesis testing ( $P_{adj}$ ) = 0.01). To optimize the stringency of potential cancer enrichment analyses, we restricted the set of viral protein targets identified by TAP-MS to those identified by three or more unique peptides, a choice corresponding to an experimental reproducibility rate greater than 90% (Supplementary Fig. 13). The resulting stringent candidate set of 947 host target genes (the 'VirHost' set; Supplementary Table 9) included 16 proteins encoded by CC genes ( $P = 0.007$ ; Fig. 4a), among which tumour suppressor genes were significantly over-represented ( $P = 0.03$ ).

As a complementary approach to validate our VirHost gene set, we compiled a list of human orthologues of mouse genes recently implicated in tumorigenesis by *in vivo* transposon mutagenesis screens<sup>25</sup>. Our VirHost data set overlaps significantly with these candidate cancer genes ( $P < 0.0001$ ) (Fig. 4b and Supplementary Table 10). The 156 candidate genes in the overlap were markedly enriched both for CC genes (odds ratio (OR) = 13,  $P = 4 \times 10^{-9}$ ) and for genes implicated in apoptosis, hypoxia response and cell growth pathways ( $P_{adj} < 0.05$  for all). Taken together, these observations suggest that our VirHost data set points to previously unknown human cancer-associated genes.

Large-scale tumour-sequencing efforts have the potential to discover new tumour suppressors and oncogenes. To explore how the VirHost data set might be used to interpret these data, we compiled somatic mutations for eight different cancers identified through 12 sequencing projects. Non-synonymous somatic mutations were reported for 10,543 genes, so further prioritization is required for useful identification of candidate causal cancer genes. We therefore scored the likely functional effects of these mutations by using the PolyPhen2 program<sup>26</sup> and generated a cumulative somatic mutation (SM) score for each protein (Supplementary Fig. 14). To compare performance in identifying candidate cancer genes of our VirHost set with that of proteins ranked by SM analysis, we tested a matching number (947) of the top-ranked SM candidates for overlap with CC genes (Fig. 4c and Supplementary Table 11). In comparison with the 16 cancer genes identified in our VirHost set, SM recovered 23 genes

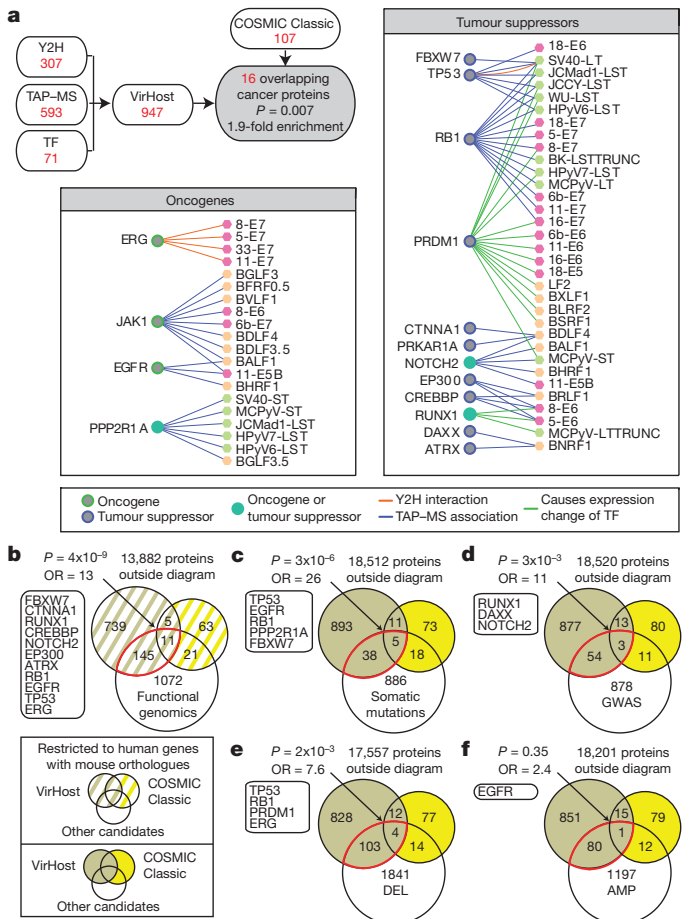


**Figure 4 | Interpreting cancer genomes with the use of virus-host network models.** **a**, Diagram describing the composition of VirHost (proteins identified by TAP-MS with at least three unique peptides, Y2H and TF) and overlap with COSMIC Classic (CC) genes. Viral protein (hexagons) perturbations of cancer proteins (circles), with cancer proteins classified as oncogenes or tumour suppressors. **b**, Venn diagram of overlaps of VirHost proteins with CC genes and candidate cancer genes identified through four transposon-based functional genomics screens. **c**, Venn diagram of overlaps of VirHost proteins with CC genes and with a prioritized set of genes found through somatic mutation analysis.  $P$  values are based on Fisher's exact test or permutation. **d-f**, Venn diagrams comparing VirHost, GWAS (**d**), SCNA-DEL (**e**) and SCNA-AMP (**f**) data sets for ability to recover COSMIC Classic genes.

( $P = 6 \times 10^{-10}$ ). Thus, viral perturbation analysis is comparable to somatic mutation sequencing for identifying cancer genes.

Although both strategies showed significant overlap with the reference CC gene set, neither by itself suffices to pinpoint causal genes with high specificity. To overcome this difficulty we exploited the orthogonal nature of the VirHost and SM sets (given  $P = 0.58$  for their overlap) by focusing on the 43 proteins at their intersection (the 'VirHostSM' subset) (Fig. 4c). In contrast with VirHost (OR = 3.7) or SM (OR = 5.8), the VirHostSM set was markedly enriched in CC proteins (five proteins, OR = 26,  $P = 3 \times 10^{-6}$ ). Pathway analysis of the 43 proteins revealed 12 proteins implicated in the GO pathway linked to 'regulation of apoptosis' (OR = 6.0,  $P_{adj} = 0.017$ ). The intersection also includes plausible contributors to cancer pathogenesis (Supplementary Fig. 15) such as the oxidative stress response transcription factor NFE2L2.

We compared the ability of VirHost to identify CC genes with two other large-scale genomic approaches: SCNA (somatic copy number alteration)<sup>27</sup> analysis of cancer genomes and GWAS (genome-wide association studies) of cancer susceptibility<sup>28</sup>. The SCNA deletions (SCNA-DEL) and amplifications (SCNA-AMP) and GWAS sets all significantly overlapped with CC genes, but with lower specificity than

the VirHost overlap with CC (OR = 1.9 for SCNA-DEL, 2.1 for SCNA-AMP, and 3.1 for GWAS, versus 3.7 for VirHost; Fig. 4d–f). The intersections of VirHost with GWAS or SCNA-DEL genes also showed enrichment for cancer genes (Supplementary Table 12). The intersection of VirHost and SCNA-DEL was enriched for genes implicated in apoptosis (GO term ‘programmed cell death’; 15 genes,  $P_{\text{adj}} = 0.022$ , OR = 4.3). Conversely, there was no synergy in the intersection of SCNA-AMP and VirHost, perhaps reflecting the preference of viral proteins in targeting tumour suppressors rather than oncogenes (Fig. 4f).

Our systems-level explorations of viral perturbations facilitate the distinction between driver and passenger mutations in cancer genome sequences. Our data indicate that *trans*-acting viral products and *cis*-acting genome variations involved in cancer converge on common pathways.

## METHODS SUMMARY

Viral ORF entry clones were generated by PCR-based Gateway recombinational cloning<sup>4</sup>. After sequence verification, viral ORFs were transferred by *in vitro* Gateway LR recombinational cloning into expression vectors for Y2H screening<sup>9</sup> and for transduction of IMR-90 cells. Y2H screens were performed against the human ORFeome v5.1 collection of about 13,000 full-length human ORFs<sup>10</sup>. Total RNA was isolated from IMR-90 cells expressing viral ORFs, and gene expression was assayed on Human Gene 1.0 ST arrays. Microarray data were analysed with R/Bioconductor. Viral proteins and associated host proteins were purified by sequential Flag and haemagglutinin immunoprecipitation and analysed by liquid chromatography–tandem mass spectrometry. Virus–host protein complex associations from two independent purifications were analysed. Pathway enrichment was analysed with FuncAssociate<sup>29</sup>. Assessment of statistical significance for overlap between gene sets was performed with Fisher’s exact test or resampling-based approaches.

Received 8 June 2011; accepted 7 June 2012.

Published online 18 July 2012.

- Vidal, M., Cusick, M. E. & Barabási, A. L. Interactome networks and human disease. *Cell* **144**, 986–998 (2011).
- Stratton, M. R. Exploring the genomes of cancer cells: progress and promise. *Science* **331**, 1553–1558 (2011).
- Gulbahce, N. *et al.* Viral perturbations of host networks reflect disease etiology. *PLOS Comput. Biol.* **8**, e1002531 (2012).
- Calderwood, M. A. *et al.* Epstein–Barr virus and virus human protein interaction maps. *Proc. Natl Acad. Sci. USA* **104**, 7606–7611 (2007).
- Shapira, S. D. *et al.* A physical and regulatory map of host–influenza interactions reveals pathways in H1N1 infection. *Cell* **139**, 1255–1267 (2009).
- Howley, P. M. & Livingston, D. M. Small DNA tumor viruses: large contributors to biomedical sciences. *Virology* **384**, 256–259 (2009).
- Foxman, E. F. & Iwasaki, A. Genome–virome interactions: examining the role of common viral infections in complex disease. *Nature Rev. Microbiol.* **9**, 254–264 (2011).
- Editorial. What is the Human Variome Project? *Nature Genet.* **39**, 423 (2007).
- Dreze, M. *et al.* High-quality binary interactome mapping. *Methods Enzymol.* **470**, 281–315 (2010).
- Lamesch, P. *et al.* hORFeome v3.1: a resource of human open reading frames representing over 10,000 human genes. *Genomics* **89**, 307–315 (2007).
- Yu, H. *et al.* Next-generation sequencing to generate interactome datasets. *Nature Methods* **8**, 478–480 (2011).
- Zhou, F. *et al.* Online nanoflow RP–RP–MS reveals dynamics of multicomponent Ku complex in response to DNA damage. *J. Proteome Res.* **9**, 6242–6255 (2010).
- Brimer, N., Lyons, C. & Vande Pol, S. B. Association of E6AP (UBE3A) with human papillomavirus type 11 E6 protein. *Virology* **358**, 303–310 (2007).
- Hanahan, D. & Weinberg, R. A. Hallmarks of cancer: the next generation. *Cell* **144**, 646–674 (2011).
- Fujita, K., Maeda, D., Xiao, Q. & Srinivasula, S. M. Nrf2-mediated induction of p62 controls Toll-like receptor-4-driven aggressive-like induced structure formation and autophagic degradation. *Proc. Natl Acad. Sci. USA* **108**, 1427–1432 (2011).
- Wu, Z. H., Shi, Y., Tibbetts, R. S. & Miyamoto, S. Molecular linkage between the kinase ATM and NFκB signaling in response to genotoxic stimuli. *Science* **311**, 1141–1146 (2006).
- Tanaka, N. *et al.* Cooperation of the tumour suppressors IRF-1 and p53 in response to DNA damage. *Nature* **382**, 816–818 (1996).
- Ranganathan, P., Weaver, K. L. & Capobianco, A. J. Notch signalling in solid tumours: a little bit of everything but not all the time. *Nature Rev. Cancer* **11**, 338–351 (2011).
- Proweller, A. *et al.* Impaired Notch signaling promotes *de novo* squamous cell carcinoma formation. *Cancer Res.* **66**, 7438–7444 (2006).
- Marcuzzi, G. P. *et al.* Spontaneous tumour development in human papillomavirus type 8 E6 transgenic mice and rapid induction by UV-light exposure and wounding. *J. Gen. Virol.* **90**, 2855–2864 (2009).
- Brimer, N., Lyons, C., Wallberg, A. E. & Vande Pol, S. B. Cutaneous papillomavirus E6 oncoproteins associate with MAML1 to repress transactivation and NOTCH signaling. *Oncogene*. doi:10.1038/ncr.2011.589 (16 January 2012).
- Calderwood, M. A. *et al.* Epstein–Barr virus nuclear protein 3C binds to the N-terminal (NTD) and beta trefoil domains (BTD) of RBP/CSL; only the NTD interaction is essential for lymphoblastoid cell growth. *Virology* **414**, 19–25 (2011).
- Klinakis, A. *et al.* A novel tumour-suppressor function for the Notch pathway in myeloid leukaemia. *Nature* **473**, 230–233 (2011).
- Forbes, S. A. *et al.* COSMIC: mining complete cancer genomes in the Catalogue of Somatic Mutations in Cancer. *Nucleic Acids Res.* **39**, D945–D950 (2011).
- Copeland, N. G. & Jenkins, N. A. Harnessing transposons for cancer gene discovery. *Nature Rev. Cancer* **10**, 696–706 (2010).
- Adzhubei, I. A. *et al.* A method and server for predicting damaging missense mutations. *Nature Methods* **7**, 248–249 (2010).
- Beroukhim, R. *et al.* The landscape of somatic copy-number alteration across human cancers. *Nature* **463**, 899–905 (2010).
- Manolio, T. A. Genomewide association studies and assessment of the risk of disease. *N. Engl. J. Med.* **363**, 166–176 (2010).
- Berriz, G. F., King, O. D., Bryant, B., Sander, C. & Roth, F. P. Characterizing gene sets with FuncAssociate. *Bioinformatics* **19**, 2502–2504 (2003).

Supplementary Information is linked to the online version of the paper at [www.nature.com/nature](http://www.nature.com/nature).

**Acknowledgements** We thank members of the Center for Cancer Systems Biology (CCSB) and J. Aster, M. Meyerson, W. Kaelin, G. Superti-Furga and S. Sunyaev for discussions, and J.W. Harper, W. Hahn, P. Howley, Y. Jacob, M. Imperiale, I. Korolnik, H. Pfister and D. Wang for reagents. This work was primarily supported by Center of Excellence in Genomic Science (CEGS) grant P50HG004233 from the National Human Genome Research Institute (NHGR) of the National Institutes of Health (NIH) awarded to M.V. (principal investigator), A.-L.B., J.A.D., E.K., J.A.M., K.M., J.Q. and F.P.R. Additional funding included Institute Sponsored Research funds from the Dana-Farber Cancer Institute Strategic Initiative to M.V.; NIH grants R01HG001715 to M.V., D.E.H. and F.P.R.; R01CA093804, R01CA063113 and P01CA050661 to J.A.D.; R01CA081135, R01CA066980 and U01CA141583 to K.M.; R01CA131354, R01CA047006 and R01CA085180 to E.K.; T32HL007208 and K08HL098361 to R.C.D.; K08CA122833 to R.B.; F32GM095284 and K25HG006031 to M.P.; Canada Excellence Research Chairs (CERC) Program, Canadian Institute for Advanced Research Fellowship and Ontario Research Fund to F.P.R.; and James S. McDonnell Foundation grant 220020084 to A.-L.B. M.V. is a ‘Chercheur Qualifié Honoraire’ from the Fonds de la Recherche Scientifique (Wallonia-Brussels Federation, Belgium).

**Author Contributions** O.R.-R., G.A., M.A.C., M.G., A.D., Ma.T., F.A., D.B., A.A.C., J.C., M.C., M.D., M.C.F., S.B.F., R.F., B.K.G., A.M.H., R.J., A.K., L.L., R.R., J.M.S., S.W., J.R.-C. and E.J. performed experiments or contributed new reagents. R.C.D., M.P., G.A., T.R., M.A., S.P., A.-R.C., C.F., N.G., T.H., J.C.M., T.R.P., S.R., Y.S., S.S., Mu.T. and J.T.W. performed computational analysis. O.R.-R., R.C.D., M.P., G.A., M.A.C., T.R., M.E.C., D.E.H., K.M., J.A.M., F.P.R., J.A.D. and M.V. wrote the manuscript. A.-L.B., R.B., E.K., M.E.C., D.E.H., K.M., J.A.M., J.Q., F.P.R., J.A.D. and M.V. designed or advised research. M.A.C., T.R., M.G., A.D., M.A., Ma.T. and S.P. contributed equally and should be considered joint second authors; D.E.H., K.M., J.A.M., J.Q., F.P.R., J.A.D. and M.V. should be considered joint senior authors; additional co-authors are listed alphabetically.

**Author Information** Microarray data were deposited in the Gene Expression Omnibus database under accession number GSE38467. Reprints and permissions information is available at [www.nature.com/reprints](http://www.nature.com/reprints). The authors declare no competing financial interests. Readers are welcome to comment on the online version of this article at [www.nature.com/nature](http://www.nature.com/nature). Correspondence and requests for materials should be addressed to J.A.M. (jarrod\_marto@dfci.harvard.edu), J.Q. (johnq@jimmy.harvard.edu), F.P.R. (fritz.roth@utoronto.ca), J.A.D. (james\_decaprio@dfci.harvard.edu) and M.V. (marc\_vidal@dfci.harvard.edu).